

Bilateral laser vision tracking synchronous inspection robotic system

Chun-lei TU¹, Xiang-dong LI¹, Jie LI², Si-cong SUN³, Xing-song WANG²

¹Special Equipment Safety Supervision Inspection Institute of Jiangsu Province, Nanjing, China

²College of Mechanical Engineering, Southeast University, Nanjing, China

³College of Power Engineering, Chongqing University, Chongqing, China

Lxd1963@163.com

Abstract: For inspecting welding seams of large-scale equipment such as storage tanks and spherical tanks, it usually cost much manpower and material, while automated testing robot can achieve fast and accurate detection. Because X-ray Flat Panel Detector is dependent on specialized automated equipment, it can greatly enhance X-ray inspection technology in large storage tanks that applying the Mecanum Omnidirectional Mobile Robot into automated weld detection. In this paper, an X-ray Flat Panel Detector based wall-climbing robotic system is developed for intelligent detecting of welding seams. The robot system consists of two Mecanum vehicles equipped with either a Flat Panel Detector or an X-ray generator and climbing on both side of the tank wall. Inspection robot can carry detector stably with reliable suction force and adapt to different surfaces. To let the X-ray Flat Panel Detector work properly, laser vision tracking system is used to ensure synchronous operation of the two robots. Some experiment was conducted and reported.

Keywords: weld Inspection; climbing robot; bilateral synchronous; nondestructive Testing

1 Introduction

In the large pressure spherical tank, due to the special nature of the operational environment, most of its stored material is flammable, explosive and toxic [1]. At the same time, the petrochemical products are highly corrosive and easy to cause corrosion to the tank, especially the inner wall of the tank surface. So it is need for regular large-scale pressure tank to make defect inspection to ensure compliance with the safe standard.

The climbing robot has developed rapidly in recent years, because the vertical wall work beyond human limits, it is also known as the extreme operating robot [2]. The wall-climbing robot is an automatic mechanism for high-altitude operation and has more and more attention. In the petrochemical enterprises, the wall-climbing robots mainly carry out inspection or painting [3] on cylindrical large tanks, cleaning and painting of buildings. In the nuclear industry, the wall-climbing robots are used to check thickness and so on.

In the study of climbing wall robots on large tanks, magnetic adsorption [4] can be used to adsorb the walls of metal materials. Figure 1 shows the climbing wall robot with four asymmetric magnetic disks on two parallel axes designed by the US Federal University [5], asymmetric structural designs can achieve better obstacle, the robot can be adsorbed and operated on the petroleum gas storage tank.

2-D laser displacement sensor through the construction of environmental maps can effectively plan the path of the

robot to achieve navigation and avoidance. Figure 2 is the United States Federal University automation and advanced control system laboratory using 2-D laser sensor to scan and locate the tank environment, the sensor uses the robot to explore the map, and use the SLAM software to establish the virtual environment to achieve route plan to the robot.

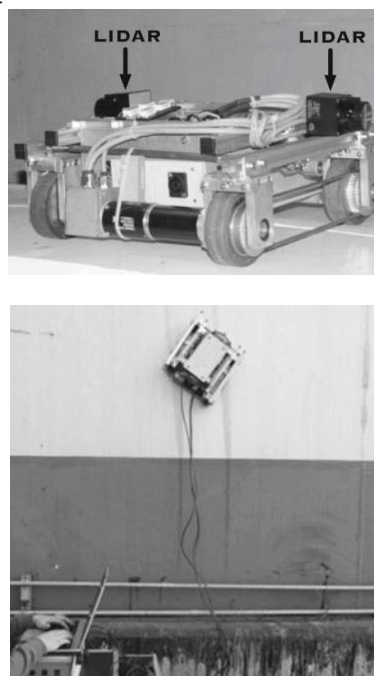


Fig.1. Tank magnetic adsorption wall climbing robot

Jiangsu Major Research and Development (Social Development) project no.BE2016802.

978-1-5386-1615-4/17/\$31.00 ©2017 IEEE

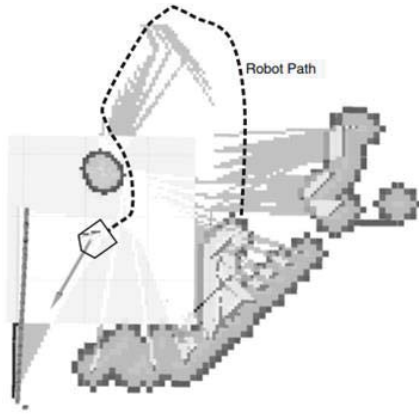


Fig.2. SLAM path planning

In this paper, the force of the climbing robot is analyzed, the climbing robot uses the laser tracking and positioning system to achieve the bilateral synchronization. The inspection robot is a wall-climbing robot that utilizes Mecanum wheel and permanent magnet adsorption to achieve adsorption and operation on the tank surface. Laser tracking and positioning system achieve tracking and positioning to the robots and establish the coordinate system to calculate the location of the two robots, the remote computer to achieve the robot synchronous movement. The remainder of this paper is organized as follows. In Section 2, the force analysis of the inspection robot is introduced. In Section 3, bilateral laser tracking and positioning system is presented. We present synchronous movement experiments and analysis of the robotic system in Section 4 and conclude the paper in Section 5.

2 Force Analysis of the Inspection Robot

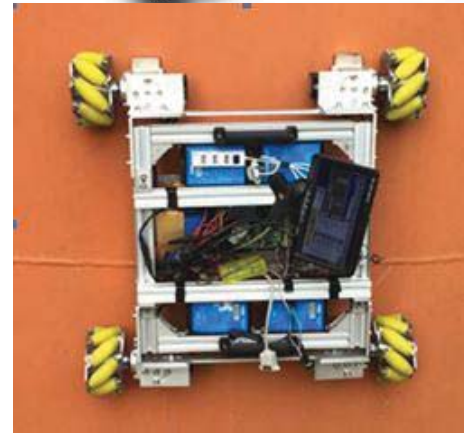


Fig.3. The inspection robot model and prototype

Figure 3 is the inspection robot model and prototype, the robot can be achieved adsorption and movement on the tank inside and outside the wall. The robot equips the Mecanum wheel [6] to achieve omnidirectional movement and use permanent magnet [7] distributed in the four wheels near to provide adsorption force.

Due to the particularity of robot work, it is necessary to analyze the force [8] of the robot. In order to simplify the analysis, the robot driving force is F_R , the friction force is F_f , and the friction force direction is opposite to the driving force [9]. The gravity of the robot is G , projected of the robot gravity on the work face is G' , $G' = G \sin \alpha$. In the following analysis, the influence of gravity to the robot mainly replaced by G' . Set along the G' direction as the Y axis, vertical of the G' direction is the X axis.

In Fig. 4, α represents the inclination angle of the work surface, β represents the angle between the driving force F_R and the gravity component G' ($G' \neq 0$) on the working surface, $0^\circ < \alpha < 360^\circ$, $0^\circ < \beta < 360^\circ$. As the angle of α and β changes, the resultant force F_a of the driving force F_R , the frictional force F_f and the gravitational force G'

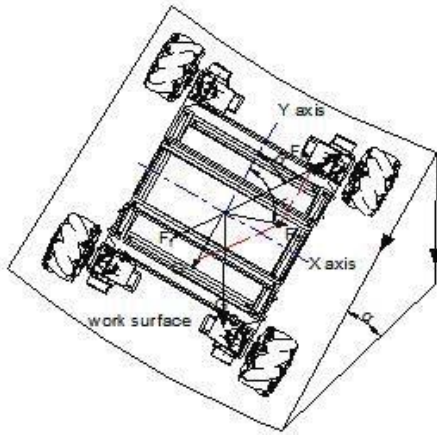


Fig.4. The force analysis of the inspection robot

will change, and the direction of F_a determines which direction the robot move.

According to the force relationship:

$$F_f = \mu(G \cos \alpha + F_c) \quad (1)$$

$$G' = G \sin \alpha \quad (2)$$

F_a in the x-axis, y-axis direction is divided into:

$$F_{ax} = (F_R - F_f) \sin \beta \quad (3)$$

$$F_{ay} = (F_R - F_f) \cos \beta - G' \quad (4)$$

F_a is:

$$\begin{aligned} F_a &= \sqrt{F_{ax}^2 + F_{ay}^2} \\ &= \sqrt{[(F_R - F_f) \sin \beta]^2 + [(F_R - F_f) \cos \beta - G']^2} \end{aligned} \quad (5)$$

Angle γ between F_a and G' is:

$$\begin{aligned} \gamma &= \arctan \left(\frac{F_{ax}}{F_{ay}} \right) \\ &= \arctan \left(\frac{(F_R - F_f) \sin \beta}{(F_R - F_f) \cos \beta - G'} \right) \end{aligned} \quad (6)$$

Substituting the above parameters, we can get the F_a and γ , when the robot moves in various positions of the sphere, providing a specific driving force F_R can control the robot on the spherical tank to all-round movement.

$$F_a = \sqrt{(A \sin \beta)^2 + (A \cos \beta - G \sin \alpha)^2} \quad (7)$$

$$\gamma = \arccos \left(\frac{A \cos \beta - G \sin \alpha}{\sqrt{(A \sin \beta)^2 + (A \cos \beta - G \sin \alpha)^2}} \right) \quad (8)$$

$$\text{And } A = F_R - \mu(G \cos \alpha + F_c) \quad (9)$$

Angle range, $0 < \gamma < \pi$.

Select a special limit position on the robot movement process and make force calculation,

When $\beta = 0^\circ$, the robot driving force F_R in the opposite direction of G' , in the following special position:

1) $\alpha = 0^\circ$, the robot moves above the horizontal plane, at this time

$$F_a = F_R - \mu(G + F_c) \quad (10)$$

2) $\alpha = 90^\circ$, the robot moves on the vertical plane,

$$F_a = F_R - \mu F_c - G \quad (11)$$

3) $\alpha = 180^\circ$, the robot moves below the horizontal plane,

$$F_a = F_R - \mu(-G + F_c) \quad (12)$$

4) $\alpha = 270^\circ$, the robot moves downward on the vertical plane,

$$F_a = F_R - \mu F_c + G \quad (13)$$

When $\beta = 90^\circ$, the robot driving force F_R direction is perpendicular to G' direction ($G' \neq 0$), the difference with the previous vertical movement, the robot does horizontal movement, In the following special position:

1) $\alpha = 0^\circ$, the robot is located at the top of the horizontal plane, G' is 0, The robot moves laterally on the horizontal plane, the size of the force is:

$$F_a = F_R - \mu(G + F_c) \quad (14)$$

2) $\alpha = 90^\circ$, at this point, the robot makes lateral movement on the vertical wall, due to the impact of gravity, γ is greater than 90° , the robot is falling, the size and direction of the force is:

$$F_a = \sqrt{(F_R - \mu F_c)^2 + G^2} \quad (15)$$

$$\gamma = \arccos \left(\frac{-G}{\sqrt{(F_R - \mu F_c)^2 + G^2}} \right) \quad (16)$$

3) $\alpha = 180^\circ$, the robot is located below the horizontal plane, G' is 0, the robot moves laterally below the horizontal plane,

$$F_a = F_R - \mu(-G + F_c) \quad (17)$$

4) $\alpha = 270^\circ$, the robot makes lateral movement on the vertical wall, due to the gravity of the robot, the robot is falling, the size and direction of the force is:

$$F_a = \sqrt{(F_R - \mu F_c)^2 + G^2} \quad (18)$$

$$\gamma = \arccos \left(\frac{G}{\sqrt{(F_R - \mu F_c)^2 + G^2}} \right) + \pi \quad (19)$$

3 Bilateral Laser Tracking and Positioning System

3.1 Laser Tracking and Synchronization Principle

Figure 5 is the laser tracking and positioning schematic diagram, Laser tracking and positioning system includes PTZ, tracking cameras, laser range finder, tracking processor unit, motor control unit. The tracking camera is used to capture the robot, and then give feedback to the control unit to follow the robot and ensure that the robot in the image center. The laser range finder [10] is used to obtain the distance between the robot and the positioning

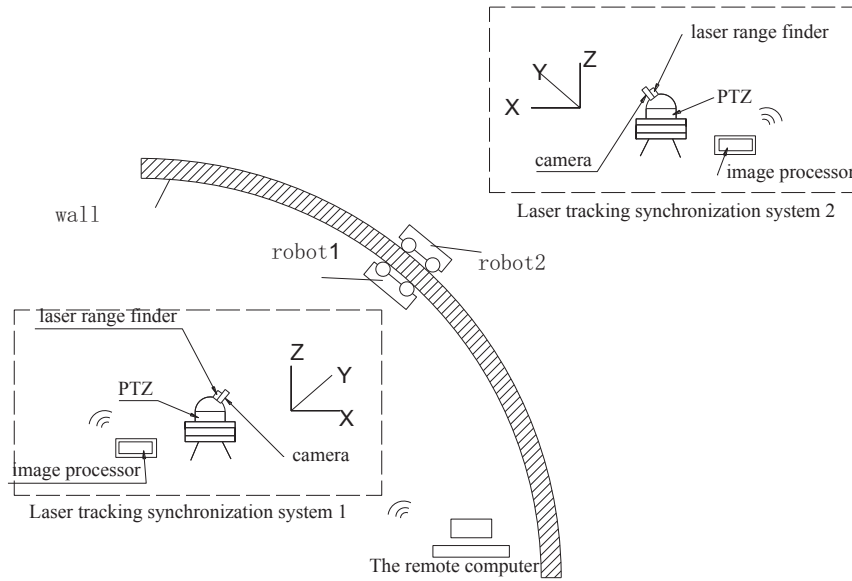


Fig.5. Laser tracking and positioning system schematic

system. Tracking processor unit and motor control unit control the PTZ rotate with 360 degrees range in the horizontal and 180 degrees in the vertical direction, and through the camera's feedback information to control the motor to ensure camera can capture the robot in real time.

The tracking processor can obtain the horizontal rotation angle α , vertical lift angle β and laser distance measurement data L and send it to the remote control center. The remote control center calculates the position difference between the two the robots and adjust the position of the robot.



Fig. 6. The tracking PTZ and industrial camera.

Laser tracking synchronization system mainly includes: stepper motor, 360 degree PTZ, camera, laser range finder, controller, and image processor and so on.

Figure 6 is the tracking PTZ and industrial camera. The PTZ adopts two stepping motors to drive the horizontal rotation through the gears and the vertical rotation through the worm gear. The camera identifies the position of the robot in the image, the stepper motor changes the horizontal and vertical angle according to the feedback data transmitted by the image to make sure the robot in the center of the image. The laser tracking synchronization system achieves bilateral robot position synchronization by acquiring both sides of the robot position

3.2 Laser Tracking Synchronization Position Calculation

After the two - side laser tracking and positioning system obtains the position parameters of the two robots, we establish the internal coordinate system 1 and the external coordinate system. Taking the cylindrical wall as an example, the coordinates of robots on both sides of the wall is shown in Figure 7.

Laser tracking and positioning system installed in the relative position on both sides of the wall, for the correct calculation, we need to measure and calibrate the initial position. The figure can be seen the center of the robot coordinates, the origin of the ambilateral coordinate system is the PTZ on both sides:

1) The internal coordinate system 1 has the diameter of the cylinder as the Z axis, the vertical line on the wall is the Y axis, and the X axis is perpendicular to the Y axis direction.

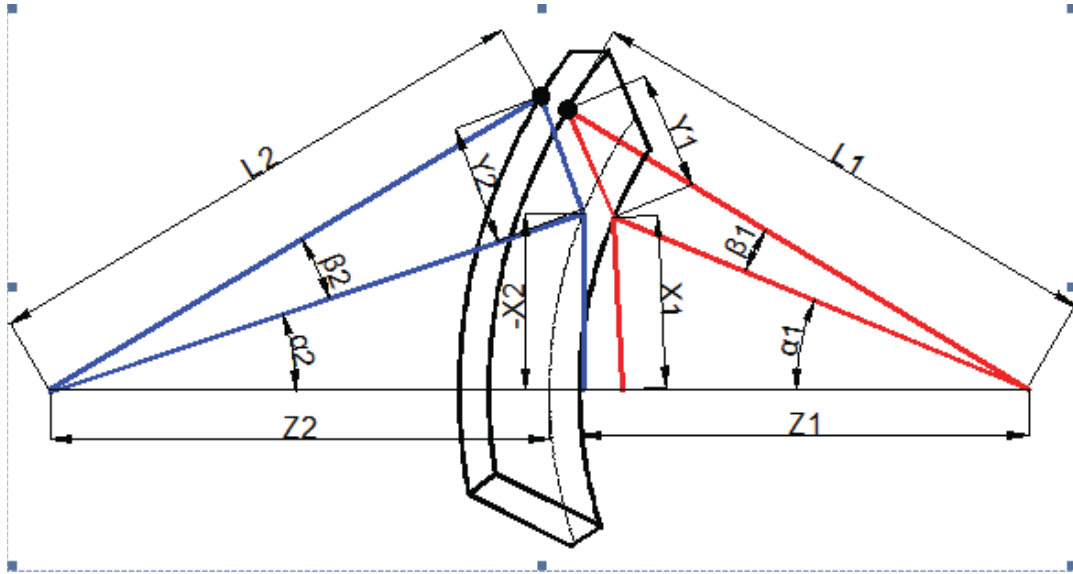


Fig.7. Robot coordinate system

2) The external coordinate system 2 has extension line of the cylinder diameter as the Z axis, the vertical line on the wall is the Y axis, and the X axis is perpendicular to the Y axis direction.

3) The Z axis is the centerline of the robot position. When the internal robot is on the left side of the Z axis, the corresponding X coordinate is negative and vice versa. The outer surface of the wall is opposite to the interior, and when the external robot is on the right side of the Z axis, the corresponding X coordinate is negative and vice versa. The Y axis is positive in the up direction and the down dip direction is negative.

Laser tracking and positioning system are in the relative position relative to the tank wall, since the wall thickness is small relative to the cylinder diameter, when the robot is synchronized on both sides, the position coordinates are simplified.

When the internal and external robot position synchronization, the coordinate relationship is:

$$X_1 = -X_2, Y_1 = Y_2 \quad (20)$$

At this time, the inside and outside robots is the same height, $Y_1 = Y_2$; in the same horizontal position, because the internal and external coordinate system relative, $X_1 = -X_2$.

Bilateral laser tracking and positioning systems achieve the robot movement tracking. The horizontal angle of the PTZ are α_1 and α_2 , the vertical angles are β_1 and β_2 , the distance of the range finder is L_1 and L_2 . The X, Y coordinates of inside and outside robot:

$$X_1 = L_1 \times \cos \beta_1 \times \sin \alpha_1 \quad (21)$$

$$X_2 = L_2 \times \cos \beta_2 \times \sin \alpha_2 \quad (22)$$

$$Y_1 = L_1 \times \sin \beta_1 \quad Y_2 = L_2 \times \sin \beta_2 \quad (23)$$

When the internal and external robot position synchronization, get:

$$L_1 \times \cos \beta_1 \times \sin \alpha_1 = L_2 \times \cos \beta_2 \times \sin \alpha_2 \quad (24)$$

$$L_1 \times \sin \beta_1 = L_2 \times \sin \beta_2 \quad (25)$$

The data obtained by the laser range finder is the actual distance, so the X and Y coordinates are the actual distance of the robot in the X and Y axes. The remote computer controls the robot 2 to synchronize the position of the robot 1 by calculating the position difference.

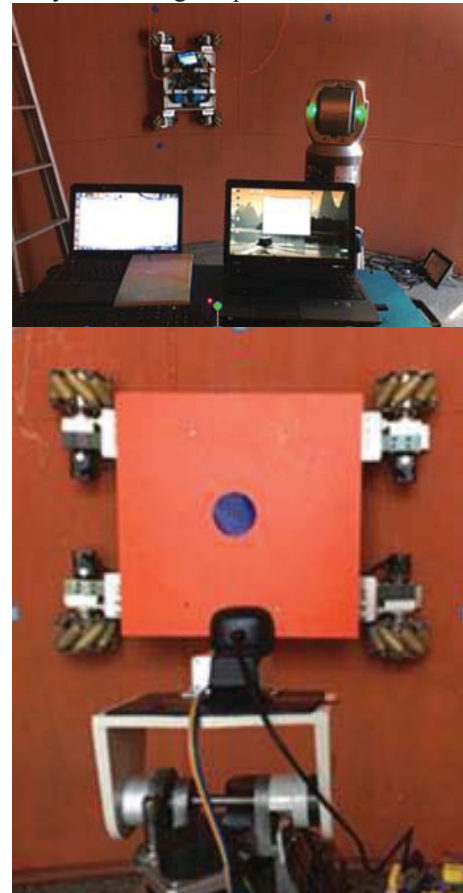


Fig. 8. Robot Synchronization Experiment

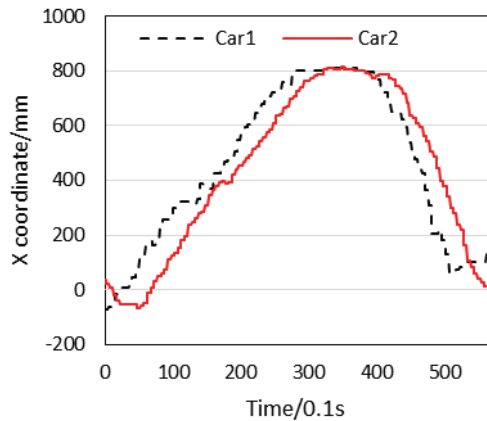
4 Experiments

The dual-car laser tracking synchronization experiment identifies and controls the PTZ to track the internal and external robots through the camera on both sides of the laser tracking device. It records the horizontal rotation angle and the vertical pitch angle of the PTZ and the laser ranging data in real time, establishes the corresponding coordinate system and calculates the double car position difference and realize the synchronization of the robots on both sides of the walls.

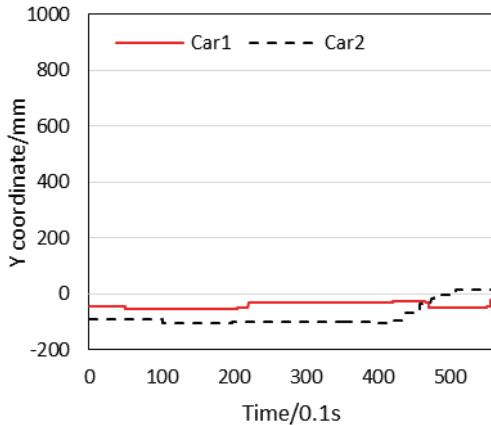
4.1 Robot Horizontal Movement Tracking

In the robot horizontal movement tracking synchronization experiment, the dual-car tracks the position by controlling the laser tracking PTZ. In the horizontal movement tracking experiment, the driving robot (CAR1) moves horizontally in the horizontal direction and the synchronization robot (CAR2) synchronizes the tracking of the active robot according to the coordinate difference.

Figure 9 shows the result of tracking when the driving robot moves horizontally. The figure shows the horizontal and ordinate data of the two robots during the whole

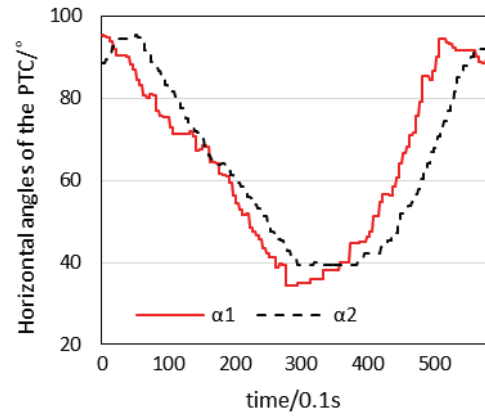


(a) X coordinate changes in horizontal movement

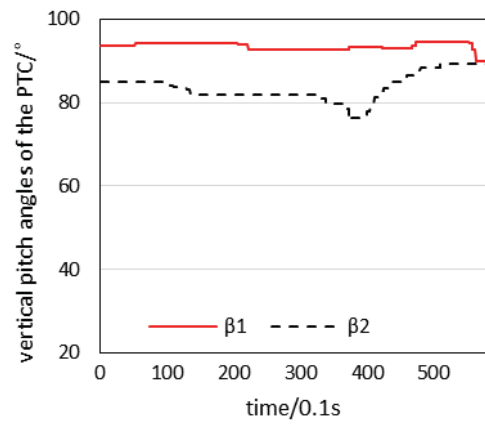


(b) Y coordinate changes in horizontal movement

Fig.9. Horizontal movement tracking synchronization



(a) Horizontal rotation angle change



(b) Vertical pitch angle change

Fig.10. Angle change of the PTZ in horizontal movement tracking

synchronization process. Figure 9 (a) shows the X coordinate change curve and (b) shows the Y coordinate change curve. It can be concluded that:

1) X coordinate gradually increase when the car is doing horizontal right shift tracking and decrease when the car is doing horizontal left shift tracking.

2) Relatively, during horizontal left and right movement, the Y coordinate change is very small and the value is basically stable.

3) In the course of the movement of dual-car X, Y coordinates difference is stable within 100mm and 10mm in the parking phase. The robot can achieve a stable tracking synchronization of position.

Figure 10(a) shows the horizontal rotation angles of the PTC α_1 and α_2 on the both sides. Figure 10 (b) shows the change in vertical pitch angles β_1 and β_2 . It can be concluded that:

1) In the process of horizontal movement tracking, it tracks the PTZ to complete the tracking and measurement of the robot. The abscissa of the robot increases first and then decreases and the horizontal rotation angle of the

PTZ turned smaller and then bigger and achieve the tracking as a result.

2) In the process of horizontal movement tracking, PTZ vertical pitch angle is stable because the robot changes little in the Y-axis direction.

4.2 Robot Longitudinal Movement Tracking

In the robot longitudinal movement tracking synchronization experiment, the driving robot (CAR1) move up and down vertically and the synchronization robot (CAR2) synchronizes the tracking of the active robot according to the coordinate difference.

Figure 11 shows the result of tracking when the driving robot moves vertically. The figure shows the horizontal and ordinate data of the two robots during the whole synchronization process. Figure 11(a) shows the X coordinate change curve and (b) shows the Y coordinate change curve. It can be concluded that:

1) The change of the X coordinate is small and there is no deviation from the vertical path when the car is doing vertical shift tracking.

2) Relatively, during the vertical movement and tracking, CAR1 move up and then down, CAR2 tracks it

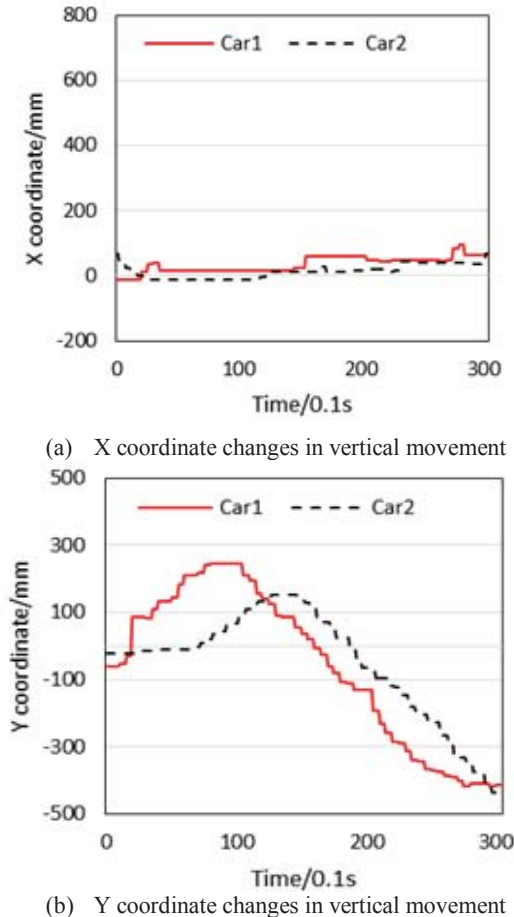
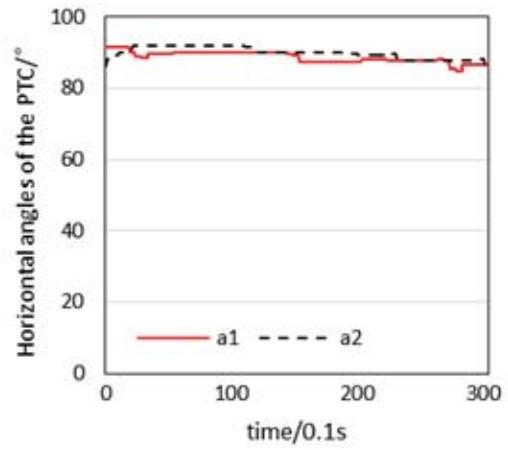
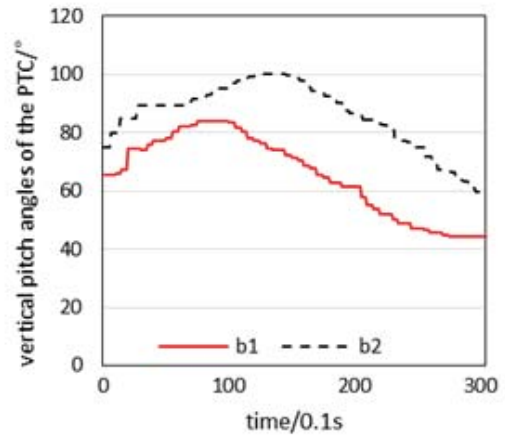


Fig.11. Longitudinal motion tracking synchronization



(a) Horizontal rotation angle change



(b) Vertical pitch angle change

Fig.12. Angle change of the PTZ in vertical tracking

quickly, Y coordinates increase first and then decrease.

3) In the course of the movement of dual-car X, Y coordinates difference is stable within 100mm and 10mm in the parking phase. The robot can achieve a stable tracking synchronization of position.

Figure 12(a) shows the horizontal rotation angles of the bilateral pan / tilt α_1 and α_2 on the both sides. Figure (b) shows the change in vertical pitch angles β_1 and β_2 . It can be concluded that:

1) During the longitudinal motion tracking, the change in the horizontal rotation angle of PTZ is small and the angle is relatively stable because change of the robot in the X-axis direction is very small.

2) During the longitudinal motion tracking, the vertical pitch angle of the PTZ is increased first and then decreased and achieve the tracking and measurement of the dual-car.

4.3 Any Direction Movement Tracking Synchronization

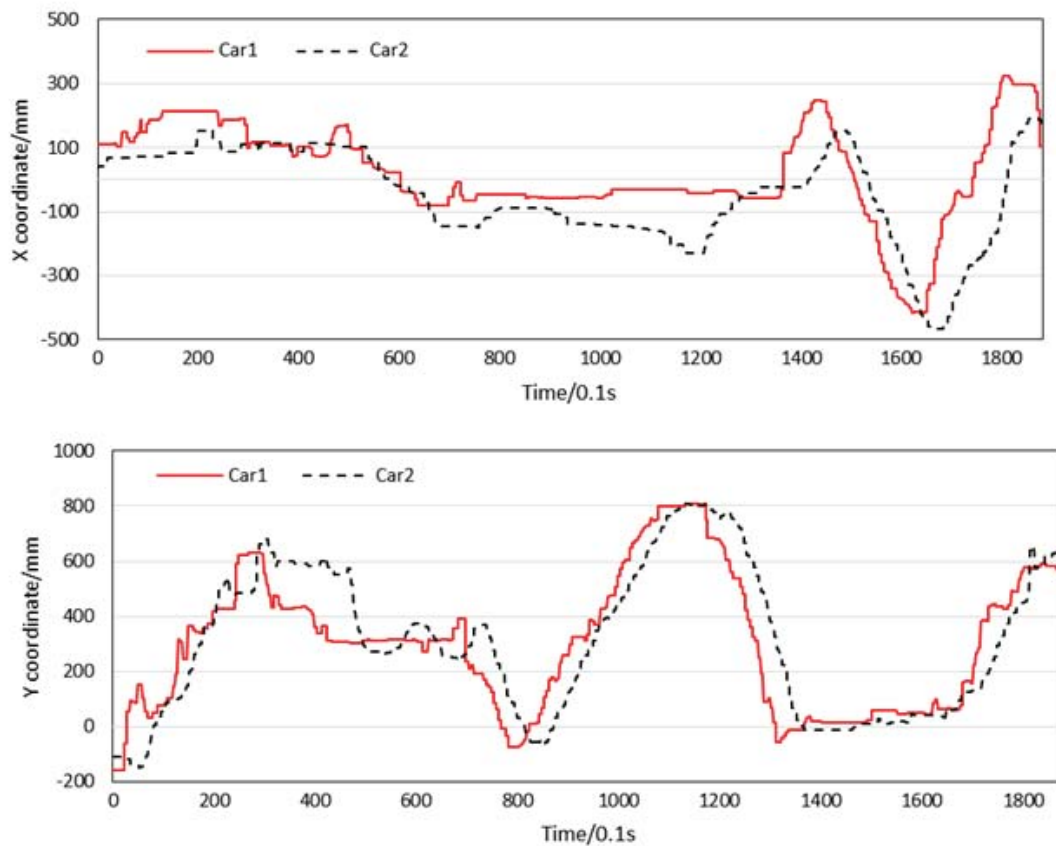


Fig.13. Laser tracking synchronous coordinate transformation on both sides

Figure 13 shows the X and Y coordinate change of the tracking when the robots move in any direction under laser tracking synchronization mode. During the synchronization process, in order to prevent the car from tracking too fast, we set the maximum speed and maximum acceleration limit and the movement of the passive robot is much smoother. The use of laser tracking can complete the dual car tracking better. Positioning accuracy is stable within 10mm in the parking phase and it can meet the X ray detection requirements [11].



(a) movement at the bottom of the tank



(b) movement on the side wall of the tank

Fig. 14 Robot field movement test

4.4 Robot Field Test and Experiment

Based on experimental platform testing, a walk and crawl test was taken on the outside of a large spherical tank in a large petrol company. The capacity of the tank is 2000 cubic meters. Diameter and wall thickness: 15700mm and 48mm, weld width: 30mm.

In the field test, the climbing robot moves smoothly. The robot can be rotated in situ and moved in any direction. The further experiment will be set in the future project research to meet the practical application.

5 Conclusions and Discussions

Climbing robot with Mecanum wheel can achieve Omni - directional movement, and the three-axis adjustable absorption mechanism we designed ensure wheels tangent to the work surface and provide sufficient adsorption force. Through the robotic force and stability analysis, the robot can make safe and reliable operation. We make some experiments and find out the influence of gravity is quite large. Through compensation to accelerate, the robot motion is more stable. More work will be performed to make the robot motion more accurate.

Acknowledgment

This partly supported by the Jiangsu Major Research and Development (Social Development) project no.BE2016802

References

- [1] Krausmann E, Mushtaq F. A qualitative Natech damage scale for the impact of floods on selected industrial facilities[J]. *Natural Hazards*, 2008, 46(2): 179-197.
- [2] Moravec H P. Robot: Mere machine to transcendent mind[M]. Oxford University Press on Demand, 2000.
- [3] La Rosa G, Messina M, Muscato G, et al. A low-cost lightweight climbing robot for the inspection of vertical surfaces[J]. *Mechatronics*, 2002, 12(1): 71-96.
- [4] Bailey S E, Olin T J, Bricka R M, et al. A review of potentially low-cost sorbents for heavy metals[J]. *Water research*, 1999, 33(11): 2469-2479.
- [5] Espinoza R V, de Oliveira A S, Valéria L, et al. Navigation's stabilization system of a magnetic adherence-based climbing robot[J]. *Journal of Intelligent & Robotic Systems*, 2015, 78(1): 65.
- [6] Diegel O, Badve A, Bright G, et al. Improved mecanum wheel design for omni-directional robots[C]//Proc. 2002 Australasian Conference on Robotics and Automation, Auckland. 2002: 117-121.
- [7] Hirose S, Tsutsumitake H. Disk rover: A wall-climbing robot using permanent[C]//Intelligent Robots and Systems, 1992., Proceedings of the 1992 IEEE/RSJ International Conference on. IEEE, 1992, 3: 2074-2079.
- [8] Spong M W, Hutchinson S, Vidyasagar M. Robot modeling and control[M]. New York: wiley, 2006.
- [9] Yoshikawa T, Zheng X Z. Coordinated dynamic hybrid position/force control for multiple robot manipulators handling one constrained object[J]. *The International Journal of Robotics Research*, 1993, 12(3): 219-230.
- [10] Teetzel J W. Laser range finding apparatus: U.S. Patent 5,669,174[P]. 1997-9-23.
- [11] Yaffe M J, Rowlands J A. X-ray detectors for digital radiography[J]. *Physics in Medicine and Biology*, 1997, 42(1): 1